Journal of New Technology and Materials
JNTM
Vol. 04, N°02 (2014)8-12

OEB Univ. Publish. Co.

Effect of thin layer thickness of iron oxide prepared by sol-gel on the opto-electronic properties of the material

M. S. Ferah[a], A. Bazine[a] and S. Sedira[b]

[a]*Laboratoire de physique chimie des semiconducteurs (LPCS), département de physique, université Constantine 1*

[b]*Laboratoire de céramiques, département de physique, université Constantine 1*

Received date: May 25, 2014; revised date: December 10, 2014; accepted date: December 21, 2014

Abstract

Thin Hematite iron oxide layers (α Fe_2O_3) were synthesized successfully using $FeCl_3$ as precursor, ethanol as solvent and acetic acid as catalyst according to the sol-gel process and spin-coating technique. The structural properties of the films were investigated by X-ray diffraction (XRD), scanning electron microscopy (SEM) and Raman spectroscopy, and optical properties by the UV-Vis spectroscopy. This study shows a singular behavior of optical transmission characterized by two bearings and a clear dependence of optoelectronic parameters with film thikness.

Keywords: Sol-Gel, iron oxide, nanomaterials, transmittance, optical constants, optical gap.

1. Introduction

The Biological or chemical water pollution has been an alarming increase in the last 50 years due to the intensification and diversification of industries. For wastewater treatment, heterogeneous photocatalysis is a process booming [1]. The materials suitable for this operation are micro and nanostructured wide bandgap semiconductors. They are oxides or sulphides of noble metals, or, more often, for reasons of cost and stability, oxides or sulphides of transition metals [1]. Among these materials, iron oxide Fe_2O_3 is a very good n type photocatalyst [2]. Its 2.1 eV gap allows a sensitivity in the visible range from 0.6 microns. With a very low price, an excellent stability and a non-toxicity under ambient conditions, Fe_2O_3 is widely used in photocatalysis, gas detection, photoelectrodes, magnetic devices and lithium batteries [3]. The sol-gel process is a chemical way very easy to implement [4], it boils down to put and properly spread a solution containing the concerned metal ion, calcining the deposit in order to remove organic compounds present in then the solution, annealing the layer to ambient air in order to ensure oxidation of the metal and crystallization of the material.

2 . Experimental

2 . 1 . Préparation of the solution

The chemicals used in preparing solutions are iron chloride hexahydrate ($FeCl_3$, 6 H_2O) 97% Aldrich as precursor, ethanol (C_2H_5OH) Aldrich 96% as solvent and acetic acid (CH_3COOH) Aldrich 99% as catalyst. The solution was prepared and synthesized at room temperature as follows: a definite quantity of each of the three products were measured in the molar proportions $FeCl_3$-ethanol-acetic acid-water : 1-225-9.5-30. The solvent is then poured into the vessel containing the solid precursor while stirring with a magnetic stirrer during half an hour.
Finally the catalyst is drip added and the solution is stirred for one hour. The solution is then ready for use.

2 . 2 . Layer déposition

The substrates used are analysis glass slides (2x1 cm) previously cut and cleaned in ultrasonic baths of acetone, methanol and distilled water for 15 minutes each time. Once dried, the substrate is fixed on the rotating part of the spin coater and then the layers are deposited at a rate of three drops for each sublayer. The rotation speed is 500 rev/min and the time 20s. Each sublayer is followed by drying at 100 °C for 10

min in a muffle furnace and, finally, the layer is annealed at 500 °C in the same oven for 1 hour. We fabricated four layers each having a different number of sublayers (table 1).

Layer	Nb sublayers
6F1	1
6F2	2
6F3	3
6F5	4

Table 1 : Number of sublayers in each sample.

2 . 3 . Analysis techniques

The morphology of the layers was analyzed by scanning electron microscopy (SEM) on a device of the type "JEOL JSM 7001F FEG SEM" with an acceleration voltage of 5-15 kV. The crystal structure was characterized by X-ray diffraction (XRD) on the diffractometer "D8 Advance AXS Brunker" in shaving mode with monochromatic radiation $CuK_{\alpha 1}$ (λ = 1,54056 Å). The characterization of the phases was made by Raman spectroscopy with the spectrometer "Bruker SENTERRA" in the range 0 to 4000 cm^{-1}. Finally, thikness and optical properties of the layers were evaluated by study of the transmission spectra in the wavelength range of UV-Visible (200-800 nm), with a double beam spectrophotometer "JASCO V670

3 . Résults and discussion

3 . 1 . Morphology

Figure 1 shows the microstructure of the surface layers Fe_2O_3.

At low magnification (x 1000), the micrograph (1a) shows an inhomogeneous deposition covering some areas and leaving others completely naked. At high magnification (x 8000) micrograph (1b) shows a structure of grain sizes of up to 200 nm.

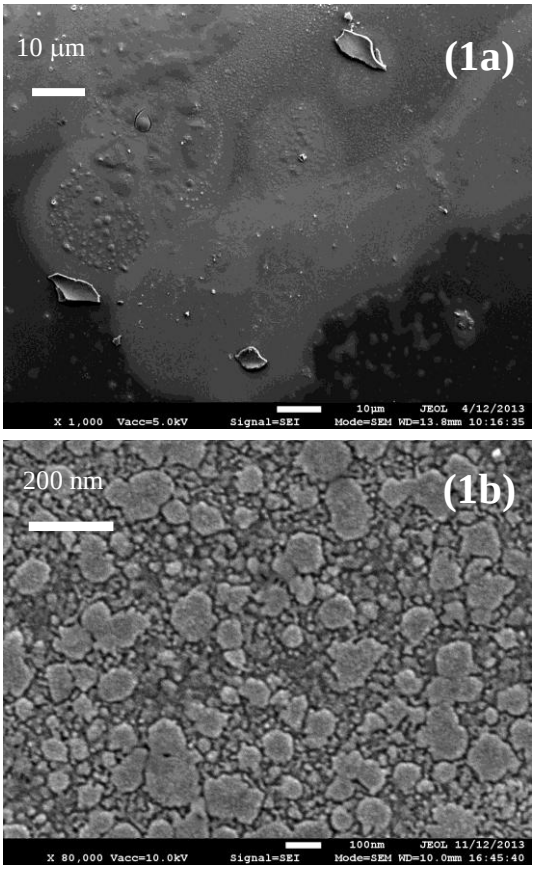

Figure 1 : SEM micrographs of Fe_2O_3 layers.

3 . 2 . Structural properties

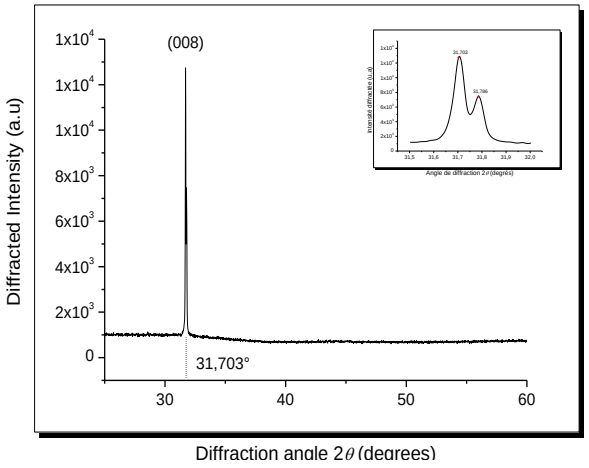

Figure 2 : XRD diffraction spectrum layers

XRD measurements of the four layers provide substantially the same record (figure 2). It consists of a single peak at $2\theta = 31.703°$. The nearest peak on

the ASTM specifications is located at $2\theta = 31.719°$ and corresponds to (008) plane of Hematite phase (α-Fe_2O_3). We therefore conclude that our material is mainly the Hematite phase (α-Fe_2O_3) of iron oxide. As for the exclusive presence of a single peak, this would mean a preferential growth along the axis perpendicular to this plane [5].

The development of this peak revealed a doublet : 31.703 ° and 31.786 °. Assuming the two peaks from the same plane, the application of the Bragg law $n\lambda = 2d\sin\theta$ gives for the second peak : $\lambda' = 1.5445$ Å corresponding to $CuK_{\alpha 2}$ line of X-ray generator.

In addition, the spectrum also allows us to estimate the average grain size D from the empirical Scherrer law [5] :

$$D = \frac{0{,}9\lambda}{\Delta\theta.\cos\theta} \qquad (1)$$

Where λ and θ are respectively the wavelength and the diffraction angle of the largest peak and $\Delta\theta$ the half-height width of this peak. The evaluation of these quantities on the diffraction pattern of Figure 2 gives : D = 170 nm.

3 . 3 . Raman Spectroscopy

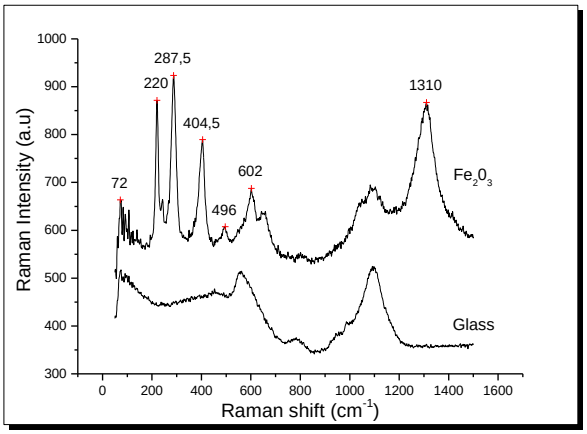

Figure 3 : Raman spectra of Fe_2O_3 layers

Figure 3 shows the typical Raman spectrum of Fe_2O_3 layers. The peaks 220; 287.5; 404.5; 496 and 1310 cm^{-1} belongs to Hematite phase [8] but are offset 5 to 7 cm^{-1} because the variation of the crystallinity and the grain size, as explains Alian et al. [6].

3 . 4 . UV-Visible spectroscopy

In figure 4 are shown the four optical transmission spectra of Fe_2O_3 layers. These spectra show a singular appearance composed of three common areas of high absorption in the UV range of 200-300 nm, low absorption in the visible range of 600-800 nm and average absorption between the two areas with a remarkable level of low absorption between 300 and 400 nm.

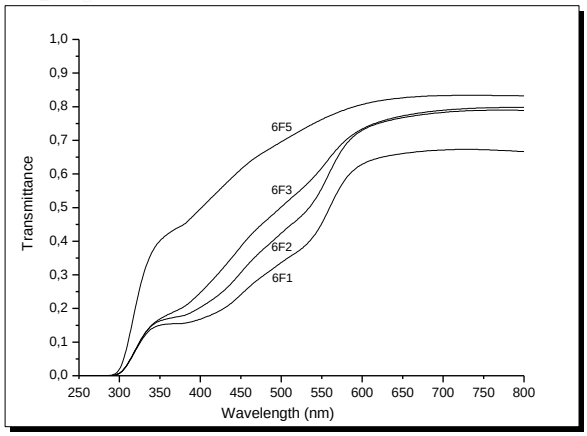

Figure 4 : Transmittance of Fe_2O_3 layers.

The transmittance of thin films obeys to the law [7]:

$$T = \frac{Ax}{B + Cx + Dx^2} \qquad (2)$$

where : $A = 16s(n^2 + k^2)$

$B = [(n+1)^2 + k^2][(n+s)^2 + k^2]$

$C = 2[-(n^2 - 1 + k^2)(n^2 - s^2 + k^2) + 4k^2 s].\cos\varphi$
$\quad - 4k[s(n^2 - 1 + k^2) + (n^2 - s^2 + k^2)].\sin\varphi$

$D = [(n-1)^2 + k^2][(n-s)^2 + k^2]$

$\varphi = 4\pi nd/\lambda$; $x = \exp(-\alpha d)$

k : Extinction index layer.

n : Refractive index layer.

s : Refractive index substrate ($s = 1.52$).

λ : Wavelenght.

d : Layer thickness.

The fit of this relationship was used to estimate the layer thicknesses and optical constants. Figure 5 shows the thicknesses depending on the number of sublayers deposited with an average of 374.5 nm in a sublayer.

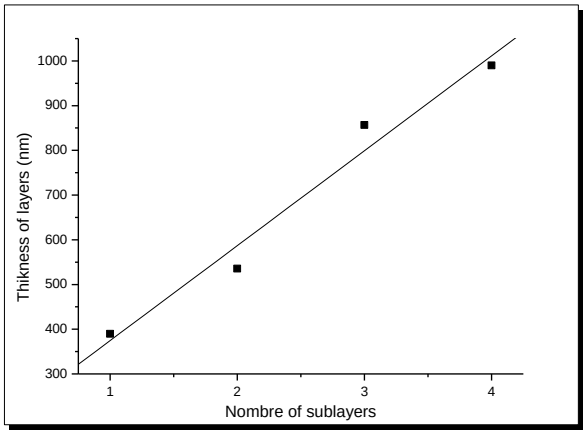

Figure 5 : Thikness of Fe_2O_3 layers.

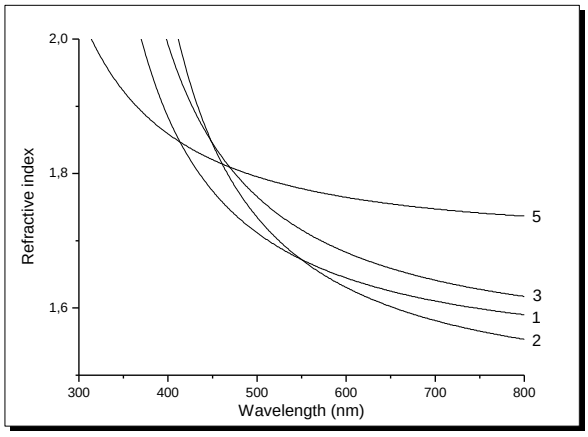

Figure 6 : Refractive index of Fe_2O_3 layers.

Figure 6 shows the variation of the refractive index as a function of wavelength. This variation shows a common appearance with very high values in the UV region of strong absorption decreases greatly in the visible range of approaching the value of 1.74 for the thickest layer.

Figure 7 shows the variation of the extinction index as a function of the wavelength. This quantity decreases rapidly from a high value in the UV to near-constant value of 0.03 in the visible.

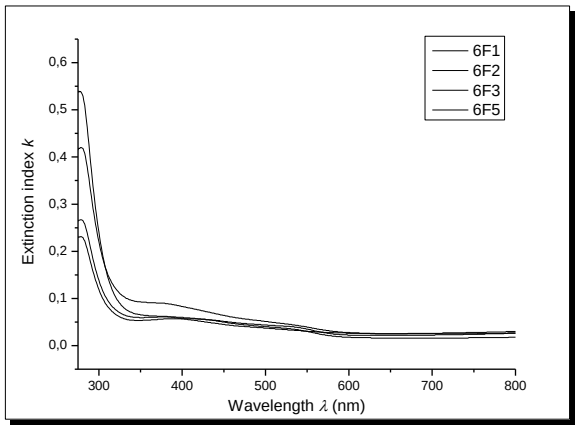

Figure 7 : Extinction index of Fe_2O_3 layers.

From this quantity we estimated the absorption coefficient α in accordance with the relationship law [7]:

$$\alpha = \frac{4\pi k}{\lambda} \qquad (3)$$

where λ is the wavelength of the incident photons.

In the region of strong absorption, this coefficient is connected to the energy of the incident photons by the Tauc relation [8] :

$$(\alpha h\nu)^m = K(h\nu - Eg) \qquad (4)$$

where Eg is the optical gap, K a constant independent of energy, and m a constant describing the transition mode gap, direct (m = 2) or indirect (m = 1/2). In practice, this law is linear over a large area of the region of strong absorption and becomes curve to approach the optimal absorption. The gap is deduced by extrapolating the linear portion to the point $\alpha = 0$.

In our case, the indirect mode seems more probable because of the gap values deduced. Indeed, in the region of low energies we meet the energy gap of the different layers (Figure 8) and note significant differences ranging from 1.19 eV for the 6F1 layer (390 nm) to 1.76 eV for the 6F3 layer (850 nm).

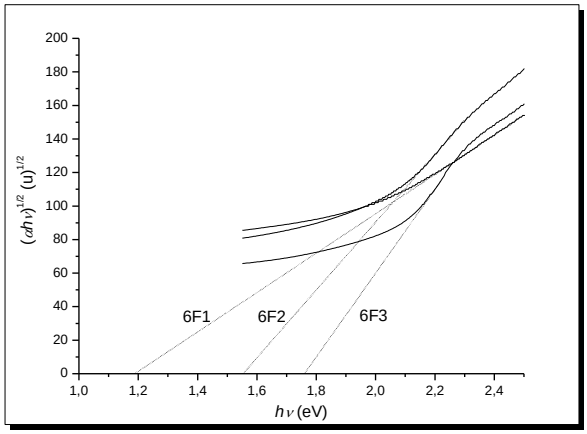

Figure 8 : Curves $(\alpha h\upsilon)^{1/2} = f(h\upsilon)$ at low energies.

These values are below the usual value 2.1 eV for Fe_2O_3 but tend to this value for larger thicknesses (Figure 9) according to an empirical exponential law of the form :

$$Eg = 2{,}054[1-\exp(-0{,}0024x)] \quad (5)$$

where x is the layer thikness.

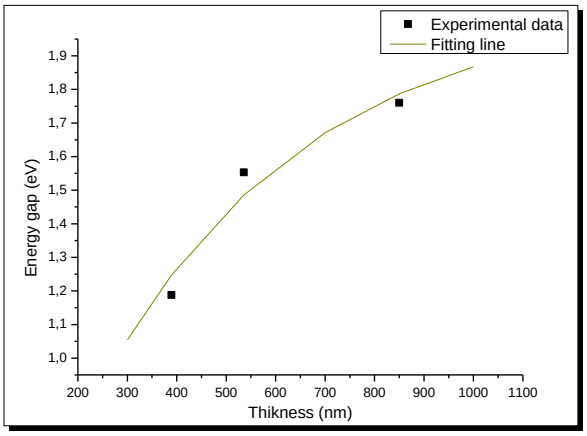

Figure 9 : Energie gap according to layer thikness.

4 . Conclusion

Thin films of Fe_2O_3 were deposited on glass substrates by the sol-gel process and spin-coating technique. SEM micrographs show a nanosized granular structure of around 170 nm. XRD spectra consist of a single peak of (008) plane of Hematite phase (α-Fe_2O_3), indicating a preferential growth perpendicular to this plane. Raman spectroscopy confirms the sole presence of Hematite phase with peaks shifted due to the nanocrystalline structure. The thickness of the layers is in accordance with the number of sublayers deposited. The optical constants n and k vary slightly depending on the thickness near normal values $n = 1.74$ and $k = 0.03$. However, the gap shows a large dependence on the layer thickness with a tendency to the usual value 2.1 eV for thick layers.

References :

[1] Saber Ahmed, M.G. Rasul, Wayde N. Martens, R. Brown, M.A. Hashib, Desalination 261 (2010) 3–18.
[2] Young Ug Ahn, Eui Jung Kimb, Hwan Tae Kimc, Sung Hong Hahn, Materials Letters 57 (2003) 4660–4666
[3] Jacques Livage, Revue Verre, Vol 6, No 5. (2000).
[4] R. Mechiakh, N. Ben Sedrine, J. Ben Naceur, R. Chtourou, Surface & Coatings Technology 206 (2011) 243–249.
[5] K.F. Konan, B. Hartiti, B. Aka, A. Ridah, K. Dakhsi, Y. Arba et P. Thevenin, Afrique Science 06 (1) (2010) 29-37
[6] Alian Wang, L. A. Haskin, and B. L. Jolliff, Dept. Earth & Planetary Sciences and the McDonnell Center for Space Sciences, Washington University, St. Louis, MO 63130. (alianw@levee.wustl.edu).
[7] J.C. Manifacier, J. Gasiot and J.P. Fillard, Journal of Physics E: Scientific Instruments 1976 Volume 9, 1002-1004
[8] L. Dghoughi, B. Elidrissi, C. Bernede, M. Addou, M. Alaoui Lamrani, M. Regragui, H. Erguig, Applied Surface Science 253 (2006) 1823–1829.

Thanks :

SEM measurements were made graciously by Gaëlle Amiri at GEMaC of St Quentin University of Versailles in France.